International Journal of Computing and Digital Systems
ISSN (2210-142X)
Int. J. Com. Dig. Sys. 9, No.6 (Nov-2020)
http://dx.doi.org/10.12785/ijcds/090608

Classical and Fuzzy Sliding Mode Control for a Nonlinear Aeroelastic System with Unsteady Aerodynamic Model

Ragoub Zahra[1], Lagha Mohand[1] and Dilmi Smain[1]

[1] *Université Blida 1, Laboratoire des Sciences Aéronautiques, Institut d'Aéronautique et des Etudes Spatiales, B.P 270, Route de Soumaa, C.P 09015, Blida, Algérie*

Received 28 Dec. 2019, Revised 12 May 2020, Accepted 1 Aug.2020, Published 1 Nov. 2020

Abstract: This paper proposes a robust solution for the design and stability of nonlinear aeroelastic airfoils of fixed-wing drones that are widely exploited in many fields such as meteorology and surveillance. Therefore, conventional sliding mode and fuzzy sliding mode control algorithms are suggested for the stabilization of a multi-input-multi-output nonlinear aeroelastic model. The aerodynamic lift and moment are expressed based on the Wagner's function for unsteady aerodynamics, and the flight dynamic model describes the plunge and pitch motions of the aircraft wing section with trailing- and leading-edge control surfaces. The selected two-degree of freedom model that includes aerodynamic and structural nonlinearities interactions, exhibits instability phenomena such as flutter and Limit Cycle Oscillations (LCOs) beyond a critical free-stream velocity. The contribution of this work is to design control algorithms in order to improve the critical flutter speed for the aeroelastic model in which unsteady aerodynamics is introduced. The control laws permit to drive the plunge displacement and pitch angle trajectories to the origin in finite time, and to guarantee a chattering-free system. The obtained results confirm that the established controllers effectively accomplish suppression of LCOs and lead the state trajectories to the origin despite nonlinearities and gust loads.

Keywords: Nonlinear Aeroservoelasticity, Sliding Mode Control, Fuzzy Logic Controller, Flutter, Limit Cycle Oscillatory, Chattering, Unsteady Aerodynamic Model, Wagner's Function.

1. INTRODUCTION

Nonlinear aeroelasticity is the study of the interactions between elastic, inertia, and aerodynamic forces applied on an aeroelastic system in a flow field, taking in account structural and aerodynamic nonlinearities that can be present in many forms [1]. These interactions lead to undesired phenomena in a form of increasing amplitude oscillations known as flutter, or constant high amplitude ones known as Limit Cycle Oscillations (LCOs); both of them cause major structural failure [1, 2].

A special focus is given to the investigation of aeroelastic modeling and flutter analysis for an aircraft or a wing in both subsonic and supersonic flows for quasi-steady or unsteady aerodynamics [3- 7]. Structural and aerodynamic nonlinearities in a subsonic unsteady flow were investigated by Lee, Price, and Wong for studying LCOs, bifurcation and chaos [3]. Later, [4, 5] analyzed nonlinear aeroelastic-wing stability in unsteady incompressible flow via the Wagner's function, combining the structural and the aerodynamic models. Iannelli, Marcos, and Lowenberg discussed a general approach for modeling an aeroelastic system with unsteady aerodynamic loads, and a unified framework of robust modeling taking in consideration the advantages of both frequency and state space modeling methods was proposed [6]. And Xiang, Yan, and Li [7] presented in detail the recent advance and challenges in aircraft nonlinear aeroelasticity for 2-D airfoils, high-aspect-ratio wings, and full aircrafts, including strip theory and vortex-lattice aerodynamic modeling methods.

In order to eliminate flutter and LCOs exposed in the mentioned studies, and to avoid their catastrophic influence on the systems structures, flutter prediction and elimination methods have to be utilized. Firstly, passive techniques based essentially on imparting more stiffness to the structure were used, but this method caused problems of weight and cost and then, the techniques of Active Flutter Suppression (AFS) took place [8]. Many active controllers were designed for aeroelastic nonlinear systems with only one control surface (Trailing Edge Control Surface TECS) [9- 12], or with both Trailing- and Leading-Edge Control Surfaces (TLECS) [13- 17]. Bruce and Jinu investigated many researchers' contributions in AFS field. They presented the development of the solutions for aeroelasticity problems through the time from passive to active ones, arriving to AFS techniques, and validated their effectiveness using LQG and LQR controllers [8]. Stability analysis for a thin triangular wing with only TECS in unsteady flow was studied in [9]. The study showed that the use of only one TECS leads to stabilization problems that have been fixed by numerical optimization. Wang, Behal and Marzocca [14] presented the recent advance in adaptive and robust control used in

E-mail: ragoubzahra@univ-blida.dz, mlagha-aerospatiale@univ-blida.dz, s.dilmi-aerospatiale@univ-blida.dz

lifting nonlinear aeroelastic wings having only one TECS or with TLECS, for quasi-steady and unsteady models in subsonic and supersonic flows. They examined the aeroelastic system response to ephemeral, steady-stained, and time-varying disturbances using state estimation, and stability analysis methods. Structural nonlinearities with unknown system parameters were investigated in [15] to design an adaptive and neural controller.

Teng [16] used the μ-method to predict robust stability of a nonlinear aeroservoelastic system with TLECS for quasi-steady aerodynamic model. This method is based on introducing uncertainties parameters to dynamic pressure, stiffness and damping. Also, Fatehi, Moghaddam, and Rahim [17] used the μ-analyses method for flutter analysis and control of a wing section with TLECS in a quasi-steady flow, by considering uncertainty parameters associated with dynamic pressure, structural stiffness and damping, and their influence on flutter and stability margins. The studies [16] and [17] showed an agreement between predicted and experimental results, but, it is noticed that the μ-method did not increase the critical flutter velocity in a significant way. Also, this method can be used only for linear systems.

The main challenges of many studies in active control field are about the controllers' robustness and the improvement of the systems' performances. For this end, Sliding Mode Control (SMC) is extensively studied and widely used [18, 19].

SMC is a special class of variable-structure systems [20]. The main advantages of SMC are its simplicity, robustness against parameters' variation, perturbations' rejection, and high accuracy [20]. In the other hand, the SMC unignorable inconvenient is known as the chattering phenomenon that has a negative influence on the system's performances and the associated actuators [21].

To overcome chattering and ensure a finite-time fast system stabilization, SMC is combined with many other controllers [21- 26]. Second order SMC was combined with the backstepping technique in [22] by adding a disturbance and uncertainty compensator term in the controller's expression, and a modified high order SMC containing a time continuous function describing nonlinearities was proposed in [23]. Both studies were effective in removing LCOs and stabilizing the system in a finite time. Liu and Wang [25] exposed many possible Classical Sliding Mode Control (CSMC) combinations, from which Fuzzy Sliding Mode Control (FSMC) is presented as a solution to have chattering-free systems. They gave also various examples of FSMC such as FSMC based on equivalent control, and SMC based on fuzzy switch-gain regulation.

Fuzzy Logic Controller (FLC) uses linguistic information and rule-based algorithms. It has a control structure which is simple and easy to design, and does not require a full knowledge of the system model [27]. It is commonly used in several domains and for different purposes [27- 30]. But, FLC depends on the human knowledge and expertise about the studied case when choosing membership functions and fuzzy rules [31]. Thus, FSMC is chosen for its ability to fulfill the needed systems' fast convergence ensured by the SMC, with the chattering suppression guaranteed by the FLC.

The main contributions of this work are:

- To introduce unsteady aerodynamics in the nonlinear aeroelastic system model using the Wagner's function. Thing that has not been investigated in the previous works in AFS field like in [22] and [23].
- To suppress LCOs with improved system performances and increased critical flutter-speed margin via the designed controllers, and to remove the chattering phenomenon completely.
- To confirm the controllers' effectiveness by exposing and discussing the obtained simulation results.

This work is organized as follows. The nonlinear aeroelastic model is established in Sect. 2. In Sect. 3, the proposed CSMC and FSMC laws are designed. Simulation results are presented in Sect. 4, and a conclusion is given in Sect. 5.

2. MATHEMATIC MODEL

Fig. 1 presents the considered prototypical aeroelastic wing section with TLECS.

The equations of motion are [13]:

$$\begin{bmatrix} m_T & m_w x_\alpha b \\ m_w x_\alpha b & I_{ea} \end{bmatrix} \begin{bmatrix} \ddot{h} \\ \ddot{\alpha} \end{bmatrix} + \begin{bmatrix} C_h & 0 \\ 0 & C_\alpha \end{bmatrix} \begin{bmatrix} \dot{h} \\ \dot{\alpha} \end{bmatrix} + \begin{bmatrix} k_h & 0 \\ 0 & k_\alpha(\alpha) \end{bmatrix} \begin{bmatrix} h \\ \alpha \end{bmatrix} = \begin{bmatrix} -L \\ M \end{bmatrix} \quad (1)$$

Where m_T is the total mass of main wing and its support structure, m_w is the mass of the main wing, b is the mid-chord distance, I_{ea} is the mass moment of inertia about the elastic axis, x_a represents the nondimensionalized distance between the center of mass and elastic axis, C_h and C_α are the plunge displacement and pitch angle structural damping coefficients, respectively, k_h and $k_\alpha(\alpha)$ are the plunge and pitch stiffness coefficients respectively, h and α are the plunge displacement and pitch angle, respectively, L and M are aerodynamic lift and moment, respectively. $k_\alpha(\alpha)$ is a nonlinear term having this expression [15]:

$$k_\alpha(\alpha) = 12.77 + 53.47\,\alpha + 1003\alpha^2 \quad (2)$$

The aerodynamic lift $L(t)$ and moment $M(t)$ acting on a 2-D wing airfoil in an incompressible unsteady flow are developed via the Wagner's function [2], and given by:

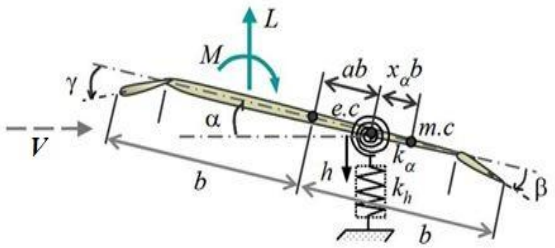

Figure 1. The aeroelastic model.

(3)

$$M(t) = \pi\rho b^3 s\left[a\ddot{h} - b\left(\frac{1}{8}+a^2\right)\ddot{\alpha} - V\left(\frac{1}{2}-a\right)\dot{\alpha}\right] + 2\pi\rho Vb^2 s\left(\frac{1}{2}+a\right)\left[\dot{h}(0) + V\alpha(0) + b\left(\frac{1}{2}-a\right)\dot{\alpha}(0)\right]\varphi(t) + 2\pi\rho Vb^2 s\left(\frac{1}{2}+a\right)\int_0^t \varphi(t-\sigma)\left[\ddot{h} + b\left(\frac{1}{2}-a\right)\ddot{\alpha} + V\dot{\alpha}\right]d\sigma + \rho V^2 b^2 s C_{m\beta}\beta + \rho V^2 b^2 s C_{m\gamma}\gamma \quad (4)$$

With ρ is the air density, V is the freestream velocity, s is the wing section surface, a is the dimensionless distance between the elastic axis and the mid-chord, β and γ are respectively the trailing- and leading-edge control surfaces deflections, $C_{l\alpha}$, $C_{l\beta}$, $C_{l\gamma}$ and $C_{m\alpha}$, $C_{m\beta}$, $C_{m\gamma}$ are the lift and the moment coefficients derivatives per α, β and γ respectively, and $\varphi(t)$ is the Wagner's function given as follows [32].

$$\varphi(t) = 1 - C_1 e^{-\varepsilon_1 (V/b)t} - C_2 e^{-(V/b)\varepsilon_2 t} \quad (5)$$

Where: $C_1 = 0.165$; $C_2 = 0.335$; $\varepsilon_1 = 0.0455$ and $\varepsilon_2 = 0.3$

In order to simplify the numerical integration of the integro-differential equations (3) and (4), another form of equations has been derived by Lee, Price, and Wong who introduced four new variables [3]:

$$L(t) = \pi\rho b^2 s[\ddot{h} - ab\ddot{\alpha}] - 2\pi\rho Vbs\left[h(0) + b\left(\frac{1}{2}-a\right)\alpha(0)\right]\dot{\varphi}(t) + 2\pi\rho Vbs\left\{\varphi(0)\dot{h} + b\left(\frac{1}{2}-a\right)\left[\varphi(0) + \frac{1}{1-2a}\right]\dot{\alpha} + \dot{\varphi}(0)h + \left[V\varphi(0) + b\left(\frac{1}{2}-a\right)\dot{\varphi}(0)\right]\alpha\right\} - 2\pi\rho Vbs[\lambda_{h_1} w_1 + \lambda_{h_2} w_2 - \lambda_{\alpha_1} w_3 - \lambda_{\alpha_2} w_4] + \rho V^2 bs C_{l\beta}\beta + \rho V^2 bs C_{l\gamma}\gamma \quad (6)$$

$$M(t) = \pi\rho b^3 s\left[a\ddot{h} - b\left(\frac{1}{8}+a^2\right)\ddot{\alpha}\right] - 2\pi\rho Vb^2 s\left(\frac{1}{2}+a\right)\left[h(0) + b\left(\frac{1}{2}-a\right)\alpha(0)\right]\dot{\varphi}(t) + 2\pi\rho Vb^2 s\left(\frac{1}{2}+a\right)\left\{\varphi(0)\dot{h} + b\left(\frac{1}{2}-a\right)\left[\varphi(0) - \frac{1}{1-2a}\right]\dot{\alpha} + \dot{\varphi}(0)h\right\} + 2\pi\rho Vb^2 s\left(\frac{1}{2}+a\right)\left\{\left[V\varphi(0) + b\left(\frac{1}{2}-a\right)\dot{\varphi}(0)\right]\alpha\right\} - 2\pi\rho Vb^2 s\left(\frac{1}{2}+a\right)[\lambda_{h_1} w_1 + \lambda_{h_2} w_2 - \lambda_{\alpha_1} w_3 - \lambda_{\alpha_2} w_4] + \rho V^2 b^2 s C_{m\beta}\beta + \rho V^2 b^2 s C_{m\gamma}\gamma \quad (7)$$

With:

$$w_1 = \int_0^t e^{-\varepsilon_1(t-\sigma)} h(\sigma)\, d\sigma \qquad w_2 = \int_0^t e^{-\varepsilon_2(t-\sigma)} h(\sigma)\, d\sigma$$

$$w_3 = \int_0^t e^{-\varepsilon_1(t-\sigma)} \alpha(\sigma)\, d\sigma \qquad w_4 = \int_0^t e^{-\varepsilon_2(t-\sigma)} \alpha(\sigma)\, d\sigma$$

And:

$$\lambda_{h_1} = C_1(V/b)\varepsilon^2{}_1 \qquad \lambda_{\alpha_1} = C_1(V/b)\varepsilon_1\left[V - \varepsilon_1 b\left(\frac{1}{2}-a\right)\right]$$

$$\lambda_{h_2} = C_2(V/b)\varepsilon^2{}_2 \qquad \lambda_{\alpha_2} = C_2(V/b)\varepsilon_2\left[V - \varepsilon_2 b\left(\frac{1}{2}-a\right)\right]$$

The state-space representation for the nonlinear aeroelastic system with unsteady aerodynamics is obtained by substituting (6) and (7) in (1), the two obtained equations are reorganized so that the nonlinear-system state representation is the following:

$$[x_1\ x_2\ x_3\ x_4\ x_5\ x_6\ x_7\ x_8]^T = [h\ \dot{h}\ \alpha\ \dot{\alpha}\ w_1\ w_2\ w_3\ w_4]^T \quad (8)$$

Where:

$$\begin{aligned}
\dot{x}_1 &= x_2 \\
\dot{x}_2 &= a_{31}x_1 + a_{32}x_3 + a_{33}x_2 + a_{34}x_4 + a_{35}x_5 + a_{36}x_6 + a_{37}x_7 \\
&\quad + a_{38}x_8 + b_{31}\beta + b_{32}\gamma \\
\dot{x}_3 &= x_4 \\
\dot{x}_4 &= a_{41}x_1 + a_{42}x_3 + a_{43}x_2 + a_{44}x_4 + a_{45}x_5 + a_{46}x_6 + a_{47}x_7 \\
&\quad + a_{48}x_8 + b_{41}\beta + b_{42}\gamma \\
\dot{x}_5 &= x_1 - \varepsilon_1 x_5 \\
\dot{x}_6 &= x_1 - \varepsilon_2 x_6 \\
\dot{x}_7 &= x_3 - \varepsilon_1 x_7 \\
\dot{x}_8 &= x_3 - \varepsilon_2 x_8
\end{aligned} \quad (9)$$

The coefficients of (9) are the following:

$$a_{31} = \left[\left[-2\pi\rho Vb^2 s\left(\frac{1}{2}+a\right)\dot{\varphi}(0)\right]B - [k_h + 2\pi\rho Vbs\dot{\varphi}(0)]C\right]/D;$$

$$a_{32} = \frac{B}{D}k_\alpha(\alpha) + G_1 - G_2;$$

$$G_1 = \left[\left[-2\pi\rho V^2 b^2 s\left(\frac{1}{2}+a\right)\varphi(0) - 2\pi\rho Vb^3 s\left(\frac{1}{4}-a^2\right)\dot{\varphi}(0)\right]B\right]/D;$$

$$G_2 = \left[\left[2\pi\rho V^2 bs\varphi(0) + 2\pi\rho Vb^2 s\left(\frac{1}{2}-a\right)\dot{\varphi}(0)\right]C\right]/D;$$

$$a_{33} = \left[\left[-2\pi\rho Vb^2 s\left(\frac{1}{2}+a\right)\varphi(0)\right]B - [C_h + 2\pi\rho Vbs\varphi(0)]C\right]/D;$$

$$a_{34} = \left[\left[C_\alpha - 2\pi\rho Vb^3 s\left(\frac{1}{4}-a^2\right)\varphi(0) + 2\pi\rho Vb^3 s\left(\frac{1}{4}-\frac{a}{2}\right)\right]B - \left[2\pi\rho Vb^2 s\left(\frac{1}{2}-a\right)\varphi(0) + \pi\rho Vb^2 s\right]C\right]/D;$$

$$a_{35} = \left[\left[2\pi\rho Vb^2 s\left(\frac{1}{2}+a\right)\lambda_{h_1}\right]B + [2\pi\rho Vbs\lambda_{h_1}]C\right]/D;$$

$$a_{36} = \left[\left[2\pi\rho Vb^2 s\left(\frac{1}{2}+a\right)\lambda_{h_2}\right]B + [2\pi\rho Vbs\lambda_{h_2}]C\right]/D;$$

$$a_{37} = \left[\left[-2\pi\rho Vb^2 s\left(\frac{1}{2}+a\right)\lambda_{\alpha_1}\right]B - [2\pi\rho Vbs\lambda_{\alpha_1}]C\right]/D;$$

$$a_{38} = \left[\left[-2\pi\rho vb^2 S\left(\frac{1}{2}+a\right)\lambda_{\alpha_2}\right]B - [2\pi\rho Vbs\lambda_{\alpha_2}]C\right]/D;$$

$$b_{31} = \left[[-\rho V^2 b^2 sC_{m\beta}]B - [\rho V^2 bsc_{l\beta}]C\right]/D;$$

$$b_{32} = \left[[-\rho V^2 b^2 sC_{m\gamma}]B - [\rho V^2 bsc_{l\gamma}]C\right]/D;$$

$$a_{41} = \left[[k_h + 2\pi\rho Vbs\dot{\varphi}(0)]B + \left[2\pi\rho Vb^2 s\left(\frac{1}{2}+a\right)\dot{\varphi}(0)\right]A\right]/D;$$

$$a_{42} = G_3 - \frac{A}{D}k_\alpha(\alpha) - G_4;$$

$$G_3 = \left[\left[2\pi\rho V^2 bs\varphi(0) + 2\pi\rho Vb^2 s\left(\frac{1}{2}-a\right)\dot{\varphi}(0)\right]B\right]/D;$$

$$G_4 = \frac{A}{D}\left[-2\pi\rho V^2 b^2 s\left(\frac{1}{2}+a\right)\varphi(0) - 2\pi\rho Vb^3 s\left(\frac{1}{4}-a^2\right)\dot{\varphi}(0)\right];$$

$$a_{43} = \left[[C_h + 2\pi\rho Vbs\varphi(0)]B + \left[2\pi\rho Vb^2 s\left(\frac{1}{2}+a\right)\varphi(0)\right]A\right]/D;$$

$$a_{44} = \left[\left[2\pi\rho Vb^2 s\left(\frac{1}{2}-a\right)\varphi(0) + \pi\rho Vb^2 s\right]B - \left[C_\alpha - 2\pi\rho Vb^3 s\left(\frac{1}{4}-a^2\right)\varphi(0) + 2\pi\rho Vb^3 s\left(\frac{1}{4}-\frac{a}{2}\right)\right]A\right]/D;$$

$$a_{45} = \left[[-2\pi\rho Vbs\lambda_{h_1}]B - \left[2\pi\rho Vb^2 s\left(\frac{1}{2}+a\right)\lambda_{h_1}\right]A\right]/D;$$

$$a_{46} = \left[[-2\pi\rho Vbs\lambda_{h_2}]B - \left[2\pi\rho Vb^2 s\left(\frac{1}{2}+a\right)\lambda_{h_2}\right]A\right]/D;$$

$$a_{47} = \left[[2\pi\rho Vbs\lambda_{\alpha_1}]B + \left[2\pi\rho Vb^2 s\left(\frac{1}{2}+a\right)\lambda_{\alpha_1}\right]A\right]/D;$$

$$a_{48} = \left[[2\pi\rho Vbs\lambda_{\alpha_2}]B + \left[2\pi\rho Vb^2 s\left(\frac{1}{2}+a\right)\lambda_{\alpha_2}\right]A\right]/D;$$

$$b_{41} = [[\rho V^2 bsc_{l\beta}]B + [\rho V^2 b^2 sC_{m\beta}]A]/D;$$

$$b_{42} = [[\rho V^2 bsC_{l\gamma}]B + [\rho V^2 b^2 sC_{m\gamma}]A]/D;$$

$A = m_T + \pi\rho b^2 s\ ; B = m_w x_\alpha b - \pi\rho b^3 sa;$

$C = I_{ea} + \pi\rho b^4 s\left(\frac{1}{8} + a^2\right); D = AC - B^2.$

3. THE PROPOSED CONTROLLERS' DESIGNS

A. *Classical sliding mode controller design*

Based on (9), the control vector *U(t)* is defined as:

$$U(t) = \begin{pmatrix} U_1 \\ U_2 \end{pmatrix} = \begin{pmatrix} b_{31} & b_{32} \\ b_{41} & b_{42} \end{pmatrix} \begin{pmatrix} \beta \\ \gamma \end{pmatrix} \quad (10)$$

Given $\boldsymbol{x_1^d}$ the desired state trajectory, $\boldsymbol{e_1}$ is the error between the actual state trajectory $\boldsymbol{x_1}$ and the desired one, and $\boldsymbol{\dot{e}_1}$ is its derivative, defined as follows:

$$e_1 = x_1 - x_1^d \quad (11)$$

$$\dot{e}_1 = \dot{x}_1 - \dot{x}_1{}^d = x_2 - x_2^d \quad (12)$$

The sliding surface in CSMC for the second order subsystem is:

$$S_1(x) = k_1 e_1 + \dot{e}_1 \quad (13)$$

k_1 is a positive scalar.

The derivative of the sliding surface is the following:

$$\dot{S}_1(x) = k_1 \dot{e}_1 + \ddot{e}_1 = k_1 e_2 + \dot{e}_2 \quad (14)$$

Given (2), we have in this case:

$$\dot{S}_1(x) = a_{31}x_1 + (k_1 + a_{33})x_2 + \left(\frac{B}{D}\,12{,}77 + G_1 - G_2\right)x_3 + \frac{B}{D}53{,}47\,{x_3}^2 + \frac{B}{D}1003\,{x_3}^3 + a_{34}x_4 + a_{35}x_5 + a_{36}x_6 + a_{37}x_7 + a_{38}x_8 + U_1 \quad (15)$$

The CSMC controller is designed as follows:

$$U_1 = U_{1eq} + \Delta U_1 \quad (16)$$

U_{1eq} is the equivalent control, where:

$$U_{1eq} = -a_{31}x_1 - (k_1 + a_{33})x_2 - \left(\frac{B}{D}\,12{,}77 + G_1 - G_2\right)x_3 - \frac{B}{D}53{,}47\,{x_3}^2 - \frac{B}{D}1003\,{x_3}^3 - a_{34}x_4 - a_{35}x_5 - a_{36}x_6 - a_{37}x_7 - a_{38}x_8 \quad (17)$$

ΔU_1 is the switching control, it provides disturbance compensation, and it has the following form:

$$\Delta U_1 = -l_1\, Sign(S_1) \quad (18)$$

l_1 is a positive scalar.

Finally, the controller expression is the following:

$$U_1 = -a_{31}x_1 - (k_1 + a_{33})x_2 - \left(\frac{B}{D}\,12{,}77 + G_1 - G_2\right)x_3 - \frac{B}{D}53{,}47\,{x_3}^2 - \frac{B}{D}1003\,{x_3}^3 - a_{34}x_4 - a_{35}x_5 - a_{36}x_6 - a_{37}x_7 - a_{38}x_8 - l_1\, Sign(S_1) \quad (19)$$

To satisfy the Lyapunov stability criterion, the Lyapunov function $V_1(x)$ and its derivative $\dot{V}_1(x)$ are considered as follows:

$$V_1(x) = \frac{1}{2}\,{S_1}^2(x) > 0 \quad (20)$$

$$\dot{V}_1(x) = \dot{S}_1(x) S_1(x) \quad (21)$$

$$\dot{V}_1(x) = S_1\,[-l_1\, Sign(S_1)\,] = S_1\left[-l_1\,\frac{S_1}{|S_1|}\right] \quad (22)$$

$$\dot{V}_1(x) = -l_1\,\frac{S_1^2}{|S_1|} < 0 \quad (23)$$

So, the Lyapunov stability criterion is satisfied for the studied aeroelastic system. In the same way, the controller for the second subsystem is obtained.

B. *Fuzzy sliding mode controller design*

Fig. 2 summarizes the fuzzy controller basic structure [26].

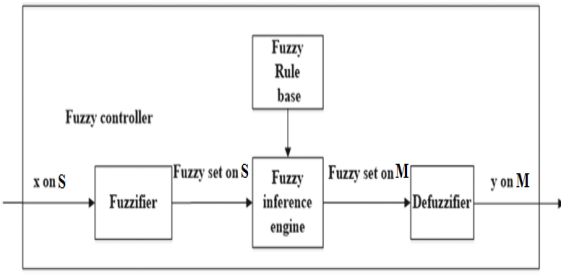

Figure 2. Fuzzy logic controller structure [26].

The idea is to design a FLC which the input is the sliding surface *S* and the output is the variant membership *M*, and to introduce the CSMC law in order to remove the chattering phenomenon [24]. The control law for the first subsystem is:

$$U_1 = U_{1eq} + M_1\,\Delta U_1 \quad (24)$$

With M_1 is the variant membership for the first subsystem.

Considering the following fuzzy sets:

- For the input S_1: *NG* (Negative and large); *N* (Negative); *Z* (Zero); *P* (Positive); *PG* (Positive and large).
- For the output M_1: *NG; N; Z; P; PG*.

The fuzzy rules are chosen as follows:

1. If S_1 is *NG* Then M_1 is *PG*
2. If S_1 is *N* Then M_1 is *P*
3. If S_1 is *Z* Then M_1 is *Z*
4. If S_1 is *P* Then M_1 is *P*
5. If S_1 is *PG* Then M_1 is *PG*

The FLC and the fuzzy rules are designed so that:

- The FSMC law is equal to the equivalent control expression if M_1 is null;
- The FSMC law is equal to the CSMC if M_1 is equal to one;
- Else, we have (24) and the chattering is reduced or eliminated via the variation of M_1.

The Lyapunov stability criterion remains satisfied since the introduced membership M_1 is always positive. In the same way, the FSMC law for the second subsystem is designed.

4. RESULTS AND COMMENTS

This part presents simulation results for plunge displacement (h) and pitch motion (alpha) for the TAMU II wing model which the parameters are given in [13].

In order to solve the differential equations of the established model, fourth order variable-step Runge-Kutta method (RK 4(5)) is adopted as the numerical method in this work. This method is commonly utilized to solve such engineering problems [33].

Fig. 3 represents pitch angle and plunge displacement time responses, under the following initial conditions $[h\ \dot{h}\ \alpha\ \dot{\alpha}\ w_1\ w_2\ w_3\ w_4]^T = [0.01\ 0\ 0.2\ 0\ 0\ 0\ 0]^T$ and for a free stream velocity of *18 m/s* beyond the open-loop critical flutter speed which is estimated at *10.7 m/s*. These results show the system instability expressed by the apparition of undesired LCOs due to structural and aerodynamic nonlinearities, which explains the importance of the active control introduction.

Under the same initial conditions, with a free stream speed of *35 m/s*, the aeroelastic system closed-loop response simulations are designed with the following CSMC parameters: $k_1 = k_2 = 1$, and $l_1 = l_2 = 5$.

Fig. 4 presents the closed-loop system responses with the trailing edge (betta β) and the leading edge (gama γ) control surfaces deflections. These deflections are limited between ± 0.5 rad (About ± 28°) in order to let their values among the actuator's physical capabilities. It can be noticed in fig. 4(a) and (b) that the established control succeeded in removing LCOs and stabilizing the system in less than a second, in spite of nonlinearities and unsteady aerodynamic loads. Fig. 4(c) and (d) show up the smooth convergence of TLECS deflections to the origin, these deflections remain within the actuator's capabilities. The sliding plane time responses are presented in fig. 4(e) and (f) which indicate that the sliding functions S1 and S2 converge smoothly and rapidly to the equilibrium position.

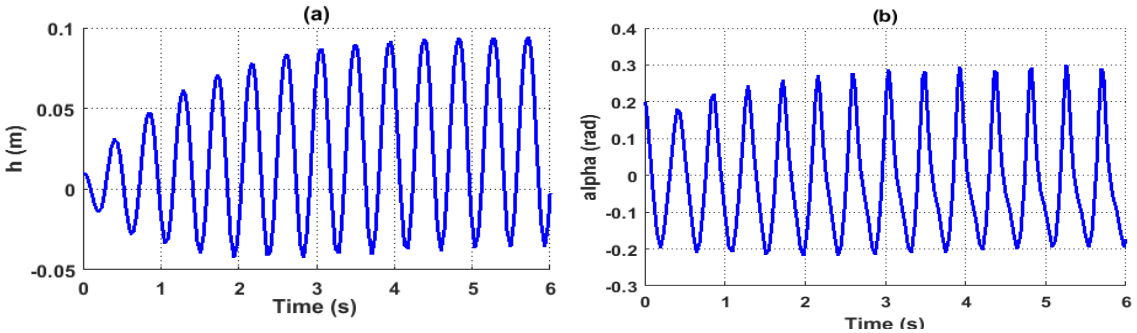

Figure 3. Open-loop time responses.

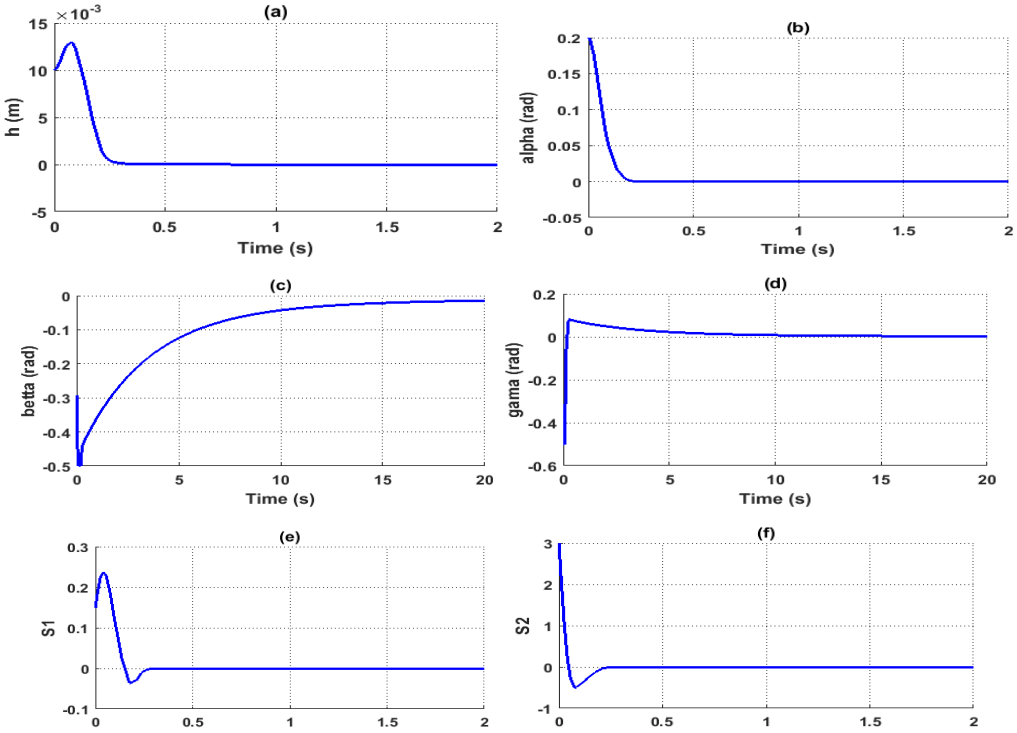

Figure 4. CSMC time responses for a wing constrained between ±0.5 rad.

Fig. 5 and fig. 6 show the system time responses behavior when the CSM controller is turned on at $t = 2\ s$ for the same closed-loop initial conditions, with a free-stream velocity of *20 m/s*. One can notice from fig. 5, that the proposed control law was able to stabilize the system when it was turned on, even after the system has entered in limit cycle oscillatory. Although, the chattering phenomenon is clearly seen in the deflections of TLECS as shown in fig. 6(a) and (b).

In order to eliminate the chattering phenomenon, CSMC law is associated with a fuzzy logic controller. The established FSMC is designed with the same CSMC parameters and for the same initial conditions.

Fig. 7 represents the closed-loop time responses for the free-stream velocity $V = 35\ m/s$, and shows that the FSMC leads to have smooth and fast stabilized system responses for high speeds. It's also noticed comparing fig. 7 and fig. 4 that FSMC maintains nearly the same system performances guaranteed by the CSMC. The memberships M_1 and M_2 time-variations are given in fig. 8(a) and (b).

The system time responses behavior and the memberships time variations when the controller is activated at $t = 2\ s$ for a speed of *20 m/s* are illustrated in fig. 9, fig. 10, and fig. 11. From these, one can remark that in addition to the quick stabilization of the system in spite of the LCOs' appearance, the introduction of the FSMC removed successfully and efficiently the chattering phenomenon appearing in the CSMC case.

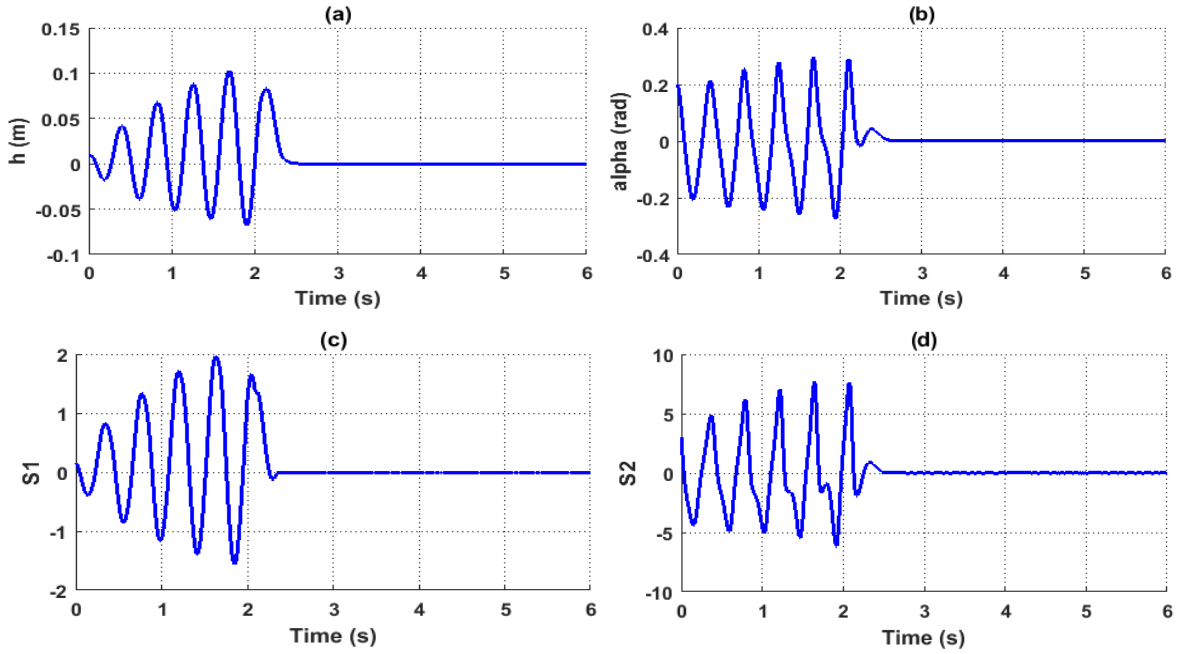

Figure 5. CSMC time responses, the controller turned on at t = 2 s.

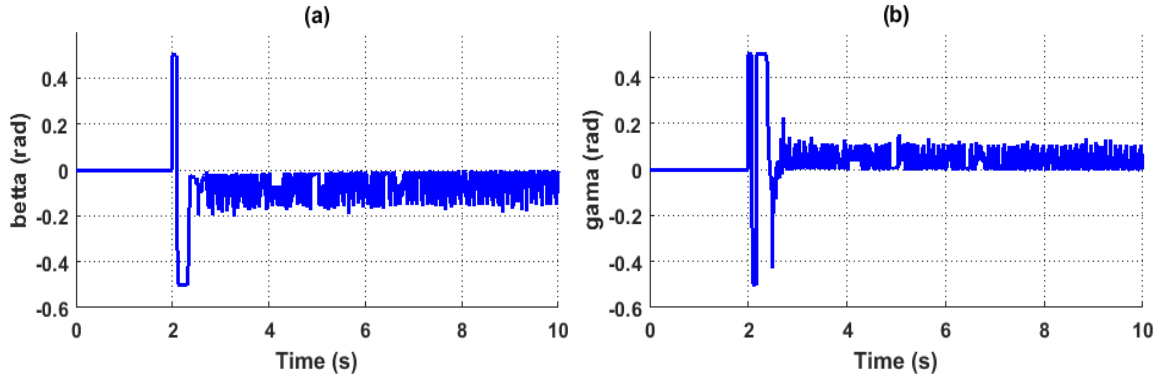

Figure 6. Chattering phenomenon in the TLECS deflections.

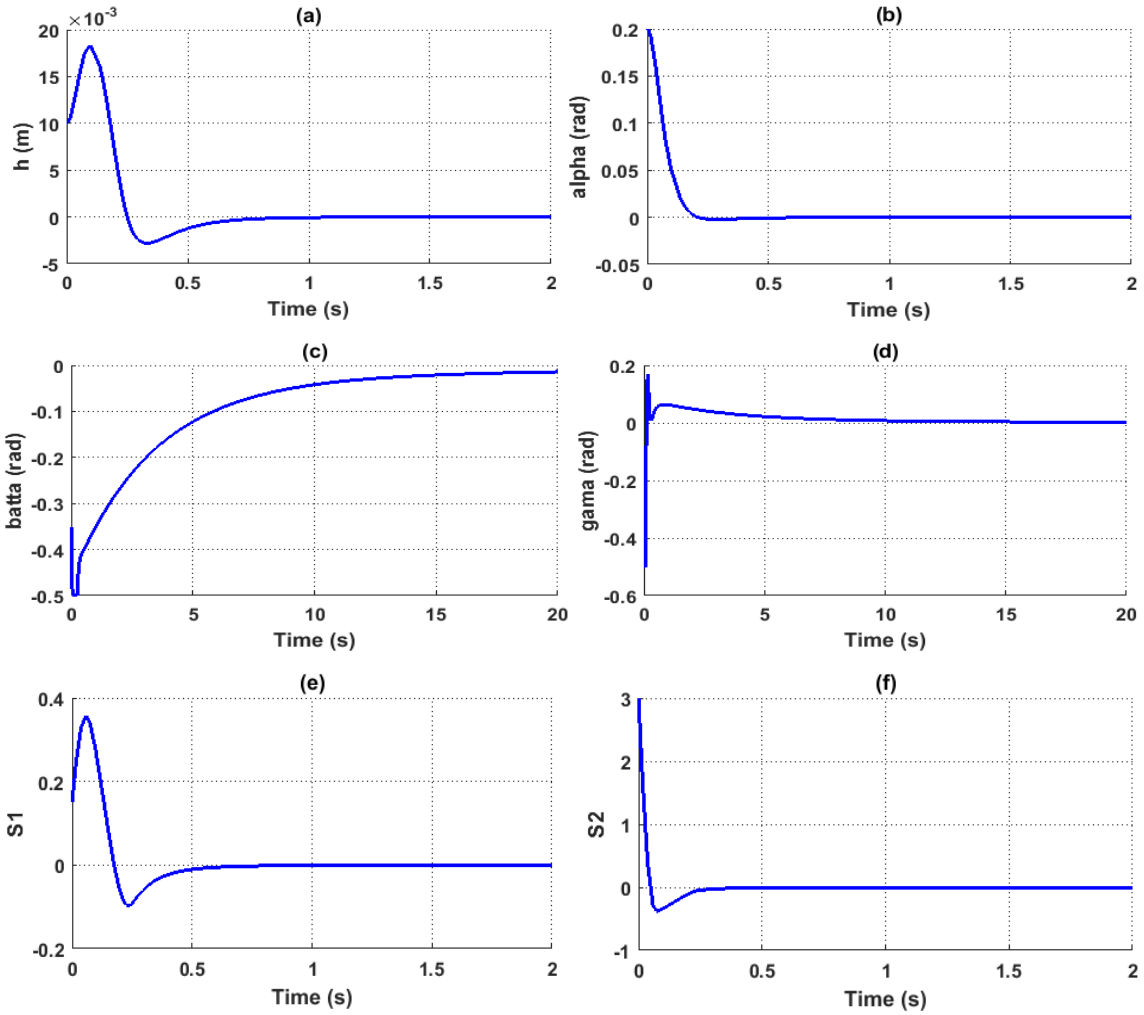

Figure 7. FSMC time responses for a wing constrained between ±0.5 rad.

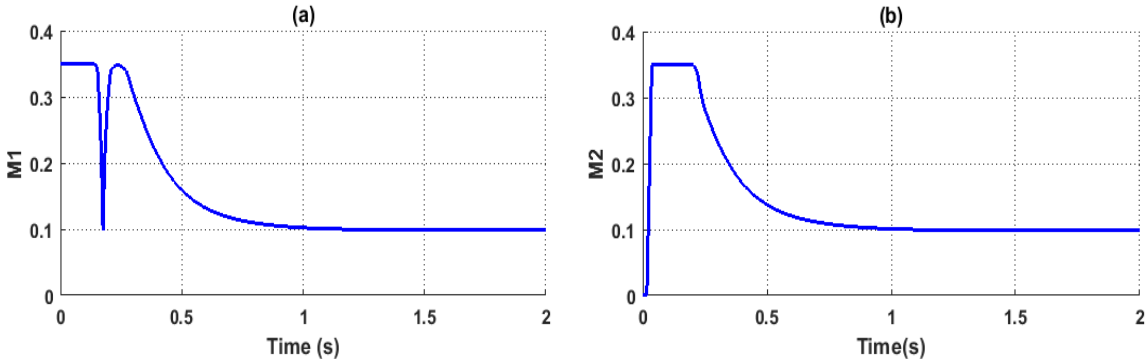

Figure 8. The memberships M_1 and M_2 time variations.

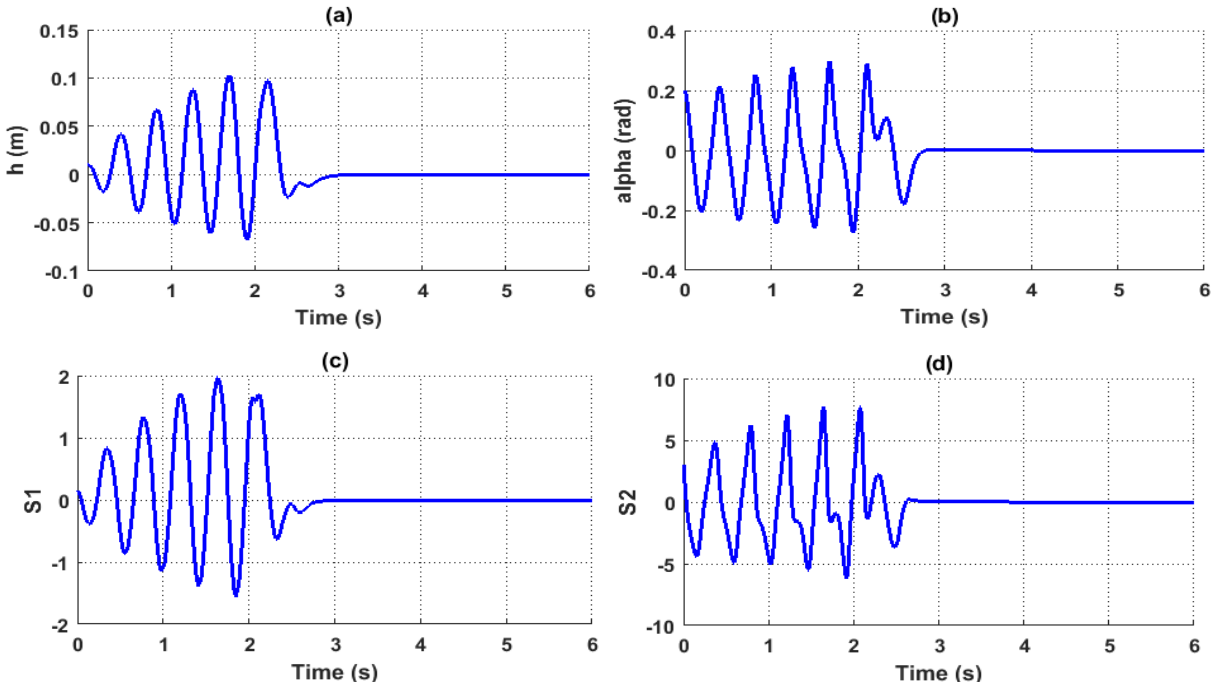

Figure 9. FSMC time responses, the controller turned on at t = 2 s.

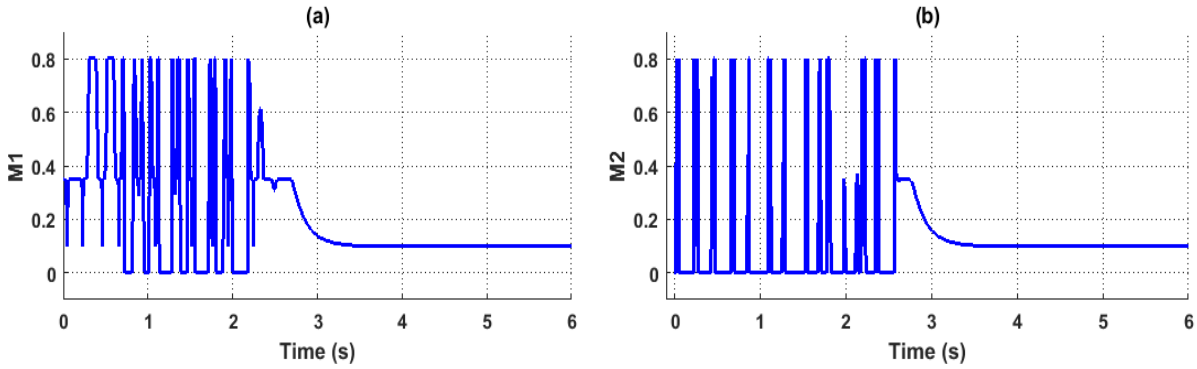

Figure 10. The memberships M_1 and M_2 time variations.

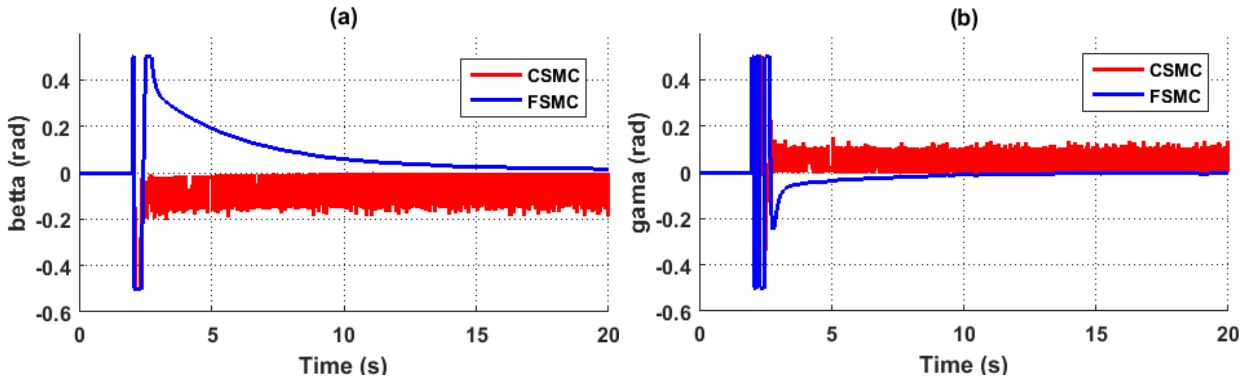

Figure 11.TLECS deflections comparison, the controller turned on at t = 2 s. Red line: CSMC, Blue line: FSMC

A comparison between CSMC and FSMC is summarized in table I.

TABLE I. A COMPARISON BETWEEN CSMC AND FSMC.

	CSMC	*FSMC*
System performances	enhanced	enhanced
Critical flutter velocity	38,27 m/s	36,99 m/s
Chaterring phenomenon	An Existing case	Removed

As can be remarked, the introduction of CSMC and FSMC leads to have a fast convergence and improved system performances in finite time. The system remains stable for speeds much higher than the open-loop flutter velocity. This means a significantly enhanced flutter-speed margin. The undesired chattering phenomenon that takes place in the CSMC case is removed using the FSMC.

5. CONCLUSIONS AND PERSPECTIVES

In this paper, a nonlinear aeroelastic airfoil with TLECS was controlled. Lift and moment were derived using the Wagner's function for unsteady aerodynamics, and a numerical application was made for the TAMU II wing model. The obtained model describes plunge and pitch motions of the wing with nonlinearity in the stiffness pitch coefficient. A CSMC and a FSMC were proposed to eliminate LCOs and to improve the system performances. The results showed that in open-loop, the system time responses exhibit dangerous LCOs beyond the critical flutter velocity. The established controllers stabilized the system smoothly and rapidly. It removed LCOs in finite time despite nonlinearities and unsteady aerodynamic loads, and improved the system performances with an important critical flutter velocity margin. The controllers were effective when they were turned on, even after the system has entered in LCO. In that case, chattering was noticed in the TLECS deflections using CSMC, but this phenomenon was completely removed using FSMC, without affecting the enhanced system performances. Things that express the robustness of the designed controllers. This may make the study a successful method in the AFS field for nonlinear aeroelastic systems with unsteady aerodynamic models, and a powerful tool to design nonlinear aeroelastic airfoils in wing tunnels in order to enhance their performances, and to solve stability problems of fixed-wing Unmanned Aerial Vehicles (UAV). Theses UAV can operate in low altitude areas, where they can undergo brutal velocity changes due to the obstacles and the turbulence existence, and in high altitude zones that can be strongly windy. This leads in most of the cases to undesired instability phenomena.

For the future works, adaptive neural SMC or genetic-algorithms based SMC can be proposed in the control field. In the conception side, the design and modeling of three-dimensional flying wings may be investigated as a perspective.

REFERENCES

[1] Y. C. Fung, ''An introduction to the theory of aeroelasticity'', Dover, USA, 1993.

[2] D. H. Hodges, G. A. Pierce, ''Introduction to structural dynamics and aeroelasticity'', Cambridge University press, New York, 2002.

[3] B.H.K. Lee, S.J. Price, Y.S. Wong, ''Nonlinear aeroelastic analysis of airfoil: bifurcation and chaos'', Prog. Aerosp. Sci. 35(3), pp 205–334, 1999.

[4] H. Haddadpour, M.A. Kouchakzadeh, F. Shadmehri, ''Aeroelastic instability of aircraft composite wings in an incompressible flow'', Composite Structures 83, pp 93-99, 2008.

[5] S.h. Shams, M.H. S. Lahidjani, H. Haddadpour, ''Nonlinear aeroelastic response of slender wings based on Wagner function'', Thin-Walled Structures 46, pp 1192– 1203, 2008.

[6] A. Iannelli, A. Marcos, M. Lowenberg, ''Aeroelastic modeling and stability analysis : A robust approach to the flutter problem'', Int J Robust Nonlinear Control 28, pp 342–364, 2018.

[7] J. Xiang, Y. Yan, D. Li, ''Recent advance in nonlinear aeroelastic analysis and control of the aircraft'', Chinese journal of aeronautics 27(1), pp 12-22, 2013.

[8] Bruce R.R.J, G.R. Jinu, ''A Study on Aeroelastic Flutter Suppression and its Control Measures - Past and Future'', International Journal of Engineering and Technology (IJET) vol 6(2), pp 960-973, 2014.

[9] D. Borglund, J. Kuttenkeuler, ''Active wing flutter suppressio using a trailing edge flap'', Journal of Fluids and Structures vol 16(3), pp 271-294, 2002.

[10] J.J. Block, T.M. Strganac, ''Applied active control for a nonlinear aeroelastic structure'', J. Guidance Control Dyn vol 21(6), pp 838– 845, 1998.

[11] J. Ko, T.W. Strganac, A.J. Kurdila, ''Stability and control of a structurally nonlinear aeroelastic system'', J. Guidance Control Dyn vol 21(5), pp 718–725, 1998.

[12] S.N. Singh, W. Yim, ''State feedback control of an aeroelastic system with structural nonlinearity'', J. Aerospace Science and Technology 7, pp 23–31, 2003.

[13] G. Platanitis, T.W. Strganac, ''Control of a nonlinear wing section using leading- and trailing-edge surfaces'', J. Guidance Control Dyn 27, pp 52–58, 2004.

[14] Z. Wang, A. Behal, B. Marzocca, ''Adaptive and Robust Aeroelastic Control of Nonlinear Lifting Surfaces with Single-Multiple Control Surfaces: A Review''. Int. J. of Aeronautical & Space Sci. vol 11(4), pp 285-302, 2010.

[15] S. Gujjula, S.N . Singh, W. Yim, ''Adaptive and neural control of a wing section using leading- and trailing-edge surfaces'', Aerosp. Sci. Technol. 9, pp 161–171, 2005.

[16] Y. Teng, ''Modeling and simulation of aeroservoelastic control with multiple control surfaces using μ- method'', University of California, USA, 2005.

[17] M. Fatehi, M. Moghaddam, M. Rahim, ''Robust flutter analysis and control of a wing'', Aircraft Engineering and Aerospace Technology vol 84(6), pp 423 – 438, 2012.

[18] S. Vaidyanathan, C-H. Lien, ''Applications of Sliding Mode Control in Science and Engineering'', Springer, Switzerland, 2017.

[19] A. R. Patel, M. A. Patel, D. R. Vyas, '' Modeling and Analysis of Quadrotor using Sliding Mode Control '', IEEE Int publishing, pp 111-114, March 2012 [44th IEEE Southeastern Symposium on System Theory, USA, 2012].

[20] Y. Shtessel , C. Edwars , L. Fridman , ''A. Levant , Sliding Mode Control and Observation, '' Springer, New York, 2014.

[21] A. Rosales, L. Ibarra, P. Ponce, and A. Molina, '' Fuzzy sliding mode control design based on stability margins,'' Journal of the Franklin Institute, vol. 356, pp 5260-5273, 2019.

[22] Z. Song, H. Li, ''Second-Order Sliding Mode Control with Backstepping for Aeroelastic Systems Based on Finite-Time

Technique'', International Journal of Control, Automation, and Systems vol 11(2), pp 416-421, 2013.

[23] S. Dilmi, B. Bouzouia, ''Improving Performance for Nonlinear Aeroelastic Systems via Sliding Mode Controller'', Arab J Sci. Eng., 2016.

[24] K. Choutri, M. Lagha, L. Dala, ''Distributed obstacles avoidance for UAVs formation using consensus-based switching topologiy,'' International Journal of Computing and Digital Systems, vol 8(2), pp 167-178, 2019.

[25] J. Liu, X. Wang, ''Advanced Sliding Mode Control for Mechanical Systems: Design, Analysis and Matlab Simulation'', Springer Heidelberg, Tsinghua University press, Beijing, 2012.

[26] F. Du, G. Li, Z. Li, Y. Sun, J. Kong, G. Jiang, and D. Jiang, '' Simulation of 2-DOF Articulated Robot Control Based on Adaptive Fuzzy Sliding Mode Control '', Springer Int publishing, pp 551-559, August 2017 [Int conf on Intelligent Robotics and Applications China, 2017].

[27] V. Kumar, S. Kumar, H. Kansal, ''Fuzzy logic controller based operating room air condition control system'', International Journal of Innovative Research in Electrical, Electronics, Instrumentation and Control Engeneering, vol **2**(01), pp 510-514, 2014.

[28] D. Harkut, and M. Ali, ''Adaptive Fuzzy Hardware Scheduler for Real Time Operating System'', International Journal of Computing and Digital Systems, vol **5**(06), pp 473-485, 2016.

[29] A. Mohammadi, S. H. Javadi, D. Ciuonzo, ''Bayesian fuzzy hypothesis test in wireless sensor networks with noise uncertainty'', Applied Soft Computing Journal, vol **77**, pp 218-224, 2019.

[30] A. Mohammadi, S. H. Javadi, D. Ciuonzo, V. Persico, A. Pescapé, ''Distributed Detection with Fuzzy Censoring Sensors in the Presence of Noise Uncertainty'', Neurocomputing, vol **351**, pp 196-204, 2019.

[31] N. Patcharaprakiti, S. Premrudeepreechacharn, Y. Sriuthaisiriwong, ''Maximum power point tracking using adaptive fuzzy logic control for grid-connected photovoltaic system'', Renewable Energie, vol **30**, pp 1771–1788, 2004.

[32] R. T. Jones, ''The unsteady lift of a wing of a finite aspect ratio'', National advisory committee of aeronautics, Report N° 681. Washington D. C., 1940.

[33] W. Y. Yang, W. Cao, T. Chung, J. Morris, ''Applied Numerical Methods Using MATLAB'', JohnWiley & Son, New Jersey, 2005.

Zahra RAGOUB was born on April the 01st 1993, in Bordj Bou Arreridj, Algeria. She received her Master diploma in avionics, on October the 07th 2017, from the Aeronautics and space studies institute of Blida 1 University - Blida, Algeria. Presently, she is a PhD student In the Aeronautics and space studies institute of Blida 1 University - Blida, Algeria. Her research activities include nonlinear aeroservoelasticity, aeroelastic modeling theories, UAV applications, control theory and robust controllers' design.

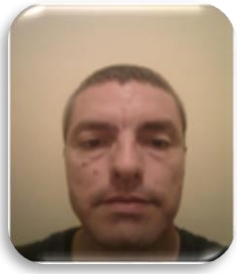

Mohand LAGHA was born in Tizi-ouzou, Algeria, on 30 June 1976. He received the Engineer Diploma in Aeronautical Engineering from the Aeronautics Institute of Blida, Algeria, in 2000, the M.Sc. in Aeronautics Sciences from the SAAD DAHLAB University of Blida, Algeria, in 2003. He received the Ph.D. degree (with honors) in Aeronautical Engineering at the Aeronautics Department of SAAD DAHLAB Blida University on 3rd July 2008, and the habilitation (HDR) on September 2010. At present he is Full Professor in Aeronautics and spatial studies Institute of Blida 1 University - Blida, Algeria. His current research activities include estimation theory, radar signal processing, weather radar signal analysis, UAV applications and Big Data Processing.

Smain DILMI is an Assistant Professor at the Aeronautics and space studies institute of SAAD DAHLAB Blida 1 University - Blida, Algeria. He received the Ph.D. degree in Aeronautical engineering from Blida 1 University in 2017. His research interests include nonlinear optimal control, robust control design, flight control, and avionics system design.

International Journal of Computing and Digital Systems
ISSN (2210-142X)
Int. J. Com. Dig. Sys. 9, No.6 (Nov-2020)

E-mail: ragoubzahra@univ-blida.dz, mlagha-aerospatiale@univ-blida.dz, s.dilmi-aerospatiale@univ-blida.dz